Tunable two-dimensional femtosecond spectroscopy

T. Brixner,* I. V. Stiopkin,* and G. R. Fleming

Department of Chemistry, University of California, Berkeley, and Physical Biosciences Division, Lawrence Berkeley National Laboratory, Berkeley, California 94720

Received September 16, 2003

We have developed a two-dimensional (2D) Fourier-transform femtosecond spectroscopy technique for the visible spectral region. Three-pulse photon echo signals are generated in a phase-matched noncollinear four-wave mixing box geometry that employs a 3-kHz repetition-rate laser system and optical parametric amplification. Nonlinear signals are fully characterized in amplitude and phase by spectral interferometry. Unlike for previous setups, we achieve long-term phase stability by employing diffractive optics and interferometric accuracy of excitation-pulse time delays by using movable glass wedges. As an example of this technique, 2D correlation and relaxation spectra at 600 nm are shown for a solution of Nile Blue dye in acetonitrile.

OCIS codes: 320.7150, 300.6290.

Ultrafast spectroscopy is increasingly turning to the study of systems that cannot be characterized by a single two-level electronic or vibrational system coupled to a bath.[1,2] Examples of such systems are the infrared spectra of peptides and proteins.[3] Accordingly, it becomes important to obtain the complete information available at a given level of the nonlinear optical response to characterize these complex systems. Two-dimensional (2D) femtosecond spectroscopy[1,2] has the potential to fully characterize the third-order nonlinear response of optical systems, and several optical four-wave mixing analogs of 2D nuclear magnetic resonance techniques have been developed.[3–10] To date 2D electronic spectroscopy has been limited to the wavelength range provided by the stable output of Ti:sapphire oscillators,[8,9] and there is a need to develop methods that are suitable for broadly tunable sources such as optical parametric amplifiers (OPAs). The required interferometric phase stability and positioning accuracy of two time delays is more difficult to achieve for shorter wavelengths, for which path-length and Poynting fluctuations lead to larger phase errors. Stability is also critical when longer acquisition times are needed for small signals from samples with scattering. Furthermore, the generation of amplified, tunable femtosecond radiation in the visible range by OPAs in general increases Poynting (and other) instabilities compared with those in stable stand-alone oscillator systems. In other applications, passive phase stabilization was achieved by use of diffractive optics (DO).[11–13] We have developed a noncollinear DO-based four-wave-mixing setup with heterodyne detection by spectral interferometry and accurate pulse-delay control by glass wedges, which for the first time to our knowledge makes possible highly stable, low-noise Fourier-transform 2D electronic spectroscopy tunable throughout the visible wavelength region.

We use a home-built Ti:sapphire regenerative amplifier laser system pumping a commercial OPA (Coherent) to generate 30-μJ, 3-kHz laser pulses (attenuated for the experiment) at 400–700 nm (~15-nm FWHM). After compression, the pulses are split into two identical parts, one of which passes through a conventional delay stage before the two parallel and equal-intensity beams enter the experimental setup (Fig. 1). The noncollinear phase-matching geometry in combination with the DO leads to inherent phase stability between the local oscillator (LO) and the emerging third-order signal field.[12,13] Two independent computer-controlled time delays are provided for pulses 1 and 2 by wedged glass plates (thickness, 1.5 mm; 1°; fused silica). Each wedge is closely paired with an identical wedge at antiparallel orientation. The stepper-driven translation is along

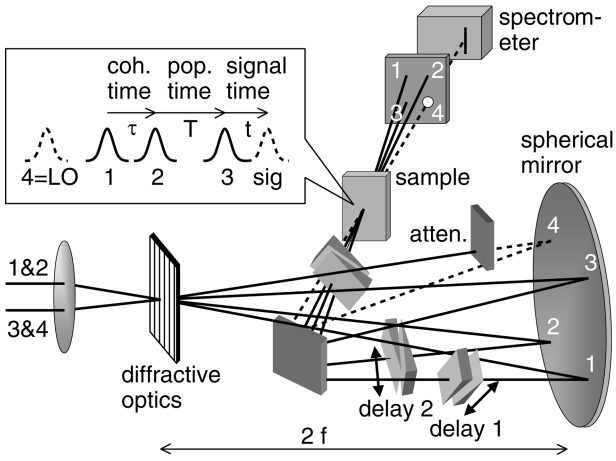

Fig. 1. Experimental setup. Two time-delayed parallel beams are focused onto a 30-groove/mm DO by a 20-cm lens. The positive and negative first diffraction orders emerge with high efficiency and provide excitation pulses 1–3 as well as the LO (4 = LO) used for heterodyne detection. A spherical mirror ($2f$ = 50 cm) generates a 100-μm beam-diameter ($1/e^2$ intensity level) image of the DO spot via a plane folding mirror inside the sample cell. Time delays (1 and 2) are introduced with interferometric precision by movable glass wedges with the required pulse orders and timing intervals τ and T (inset). Spectral interferometry between the attenuated LO and the emitted third-order signal field (dashed curves in the inset and dashed lines in the main figure) fully characterizes the response of the sample in amplitude and phase.

0146-9592/04/080884-03$15.00/0

the inner surface, whereas the outer surfaces are aligned perpendicular to the transmitted laser beam. In this way, no beam displacement occurs when any of the wedges is moved, and the total configuration in effect simply acts as a glass plate of varying thickness. A lateral translation of 1 mm corresponds to a time delay of 27 fs that, with a positioning repeatability of 100 nm, leads to a nominal delay precision of 2.7 as over a total range of 400 fs. For comparison, the time drift reported for conventional 800-nm oscillator experiments was 0.1 fs over 20 min, and with the help of continuously recorded reference interferograms followed by numerical rephasing this error was reduced to 40 as.[2] For our calibration we recombine beams 1 and 2 collinearly by setting a second (identical) DO at the sample position. Spectral interferograms are recorded with a 0.3-m imaging spectrograph and a 16-bit, 256 × 1024 pixel, thermoelectrically cooled CCD array. Temporal oscillations are analyzed by a sliding-window fast Fourier transform, which determines the calibration factor (translation versus time delay) as a function of wedge position. Hence, systematic variations in the glass thickness can easily be compensated for. However, because the relative standard deviation of the calibration factor was only 10^{-4}, a single calibration constant was used for each one of the wedges. Beam 3 passes through a fixed but otherwise identical double-wedge combination.

The LO (beam 4) passes through a neutral-density filter that attenuates the intensity by 3–4 orders of magnitude before the beam hits the sample. Additionally, the time ordering (Fig. 1, inset) is such that pulse 4 always arrives first (600 fs before pulse 3). This ensures that neither is the LO pump–probe contaminated nor does it influence the response of the molecular system. In other implementations of 2D spectroscopy the LO is recombined with the signal field after the sample.[2–9] In our geometry the LO may be modified by sample absorption and dispersion. However, any effect that this has on spectral intensity is exactly canceled during data analysis because the LO spectrum is divided out to generate the signal intensity from the complex-valued heterodyne field (see below). The modified LO phase is measured in a separate experiment by spectral interferometry and subtracted from the recovered signal field. In this way our method also determines the signal as it exits the sample, but most importantly it avoids conventional beam splitters and delay lines, thus exploiting the full phase stability of the DO.

For any given population time T, we scan coherence time τ by moving pulse 1 from $-(\tau + T)$ to $-T$ and then moving pulse 2 from $-T$ to $-(\tau + T)$. Complete determination of the four-wave mixing signal is carried out by spectral interferometry[14–17] between the signal field and the LO. Data analysis involves Fourier transformation of the spectral fringe pattern, isolation of the heterodyned signal component at positive times, inverse Fourier transformation to produce a complex-valued frequency-dependent function, and division by the LO field to get the nonlinear signal in amplitude and phase.[14,18] The shape of pulses 1–4 was recorded by second-harmonic generation–frequency-resolved optical gating[19] at the sample position with a 30-μm β-barium borate crystal. Quantitative analysis revealed near-transform-limited pulses of 41-fs duration at 595 nm (bandwidth product, 0.57), so the input phases were not included in the data analysis.[9]

The results of this spectroscopy are two-dimensional spectra:

$$S(\omega_\tau, \omega_t, T) \sim \mathrm{FT}[\exp(i\omega_0\tau - i\omega_0 t)R^{(3)}(\tau, T, t)] \quad (1)$$

in the impulsive limit (for finite pulse durations additional convolution integrals appear[1,2,9,20]), where FT indicates 2D Fourier transformation with respect to τ and t, $R^{(3)}(\tau, T, t)$ essentially contains the third-order response function of the investigated system, and ω_0 is the central laser frequency. The transformation with respect to t is already implicit in the frequency-domain detection technique, whereas the transformation with respect to τ is carried out explicitly. The overall absolute phase can be determined by comparison with spectrally resolved pump–probe spectra.[2,9] Note that the slowly varying response function is multiplied by fast oscillating phase terms that depend on exact time delays. This is the reason why precise timing is necessary for reliable 2D data. In conventional setups, artifacts caused by imperfect timing have been observed,[8] whereas the DO-based technique guarantees clean signal traces directly from the raw data.

As an example of our technique, we investigated a solution of the dye molecule Nile Blue in acetonitrile[21,22] (two electronic states coupled to vibrational modes) at a wavelength of 595 nm. The smooth structure of the spectral interferograms collected for different τ (2-fs steps) and fixed $T = 0$ fs (Fig. 2a) demonstrates the high phase stability of the setup and the timing precision of the glass wedges. Excellent phase stability and repeatability from scan to scan is illustrated in Fig. 2b, showing typi-cal interferograms for identical positions at $\tau = 0$ fs and $T = 0$ fs but recorded within separate scans 5 min apart. The fringe positions as well as their intensities are very well reproduced. The Fourier evaluation yields 2D electronic correlation (Fig. 3a; $T = 0$ fs) and relaxation spectra (Fig. 3b; $T = 100$ fs) located near $\omega_\tau \approx -\omega_0$ and $\omega_t \approx \omega_0$ owing to the phase factors in Eq. (1). At

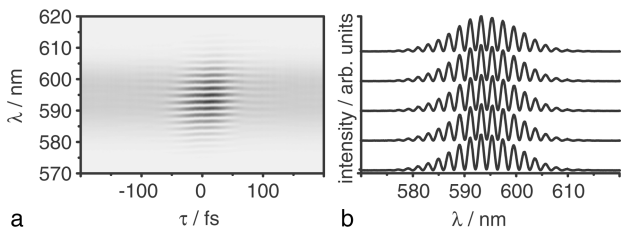

Fig. 2. a, Spectral interferograms for Nile Blue dye in acetonitrile recorded for various coherence times τ and fixed population time $T = 0$ fs. The high quality of the fringe patterns demonstrates the phase stability of the passively phase-locked setup. b, Five interference spectra for fixed $\tau = 0$ fs and $T = 0$ fs (taken from different continuous scans within 30 min) show the high phase stability and repeatability, as fringe positions and intensities are reproducible.

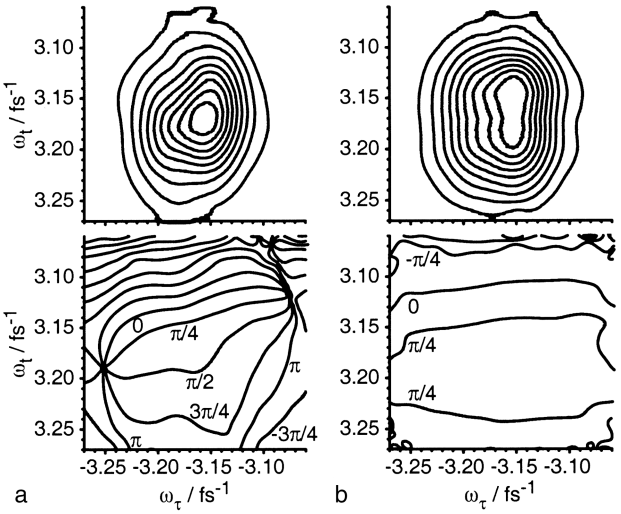

Fig. 3. 2D Fourier-transform spectra for a, $T = 0$ fs and b, $T = 100$ fs in magnitude (top) and phase (bottom) at 595-nm excitation wavelength. Contour lines are drawn in steps of 10% for the magnitude and $\pi/4$ for the phase. With increasing T, loss of memory of the initial transition frequency is seen in the lines of constant phase leveling off and in the increased symmetry of the absolute value about the vertical axis. The maximum of the absolute value at $T = 100$ fs is 60% of the peak value at $T = 0$ fs. The vertical elongation of the magnitude indicates a time-dependent Stokes shift, i.e., motion of excited-state wave packets.

$T = 0$ fs, the diagonal elongation of the absolute-value plot and the diagonal lines of constant phase indicate static disorder. For longer population times a vertical elongation of the absolute-value graph corresponds to a time-dependent Stokes shift, and the phase lines' leveling off indicate that the system is losing memory of the initial transition. This behavior is qualitatively reproduced by simulations based on a Brownian oscillator model with parameters determined previously.[21,22] Because of the stability of the setup, the background amplitude level in the 2D plots outside the region of Fig. 3 is less than 2% of the peak value (after the 2D traces from five separate scans are averaged). The pulse broadening that results from using glass wedges as delay generators is negligible (a factor of 1.0002 moving from $\tau = 0$ fs to $\tau = 300$ fs). Numerical compensation of the delay-dependent dispersive phase in the frequency-domain signal field leads to 2D graphs that are indiscernible from those in Fig. 3. The introduction of chirp is therefore insignificant.

In summary, we have demonstrated a new technique for the determination of 2D electronic correlation and relaxation spectra in the visible region. We achieved long-term interferometric phase stability and reproducibility even with the OPA output from an amplified kilohertz-repetition-rate femtosecond laser system; this allows us to analyze small signals that require long data acquisition times. In a molecular aggregate sample with scattering present, we recorded 2D spectra for which the pulse energy of the echo signal even at the maximum was below 100 aJ. The extension of this technique to ultrabroadband light sources (noncollinear OPAs) will permit measurement of the third-order response functions of complex systems that cover several electronic transitions.

This research was supported by a grant from the National Science Foundation. We thank Y.-Z. Ma for enlightening discussions and for his contributions to the experimental setup. T. Brixner thanks the German Science Foundation for an Emmy-Noether Fellowship. G. R. Fleming's e-mail address is grfleming@lbl.gov.

*Both authors contributed equally to this work.

References

1. S. Mukamel, Annu. Rev. Phys. Chem. **51,** 691 (2000).
2. D. M. Jonas, Annu. Rev. Phys. Chem. **54,** 425 (2003).
3. M. C. Asplund, M. T. Zanni, and R. M. Hochstrasser, Proc. Natl. Acad. Sci. USA **97,** 8219 (2000).
4. L. Lepetit and M. Joffre, Opt. Lett. **21,** 564 (1996).
5. N. Belabas and M. Joffre, Opt. Lett. **27,** 2043 (2002).
6. O. Golonzka, M. Khalil, N. Demirdoven, and A. Tokmakoff, Phys. Rev. Lett. **86,** 2154 (2001).
7. M. Khalil, N. Demirdoven, and A. Tokmakoff, Phys. Rev. Lett. **90,** 047401 (2003).
8. J. D. Hybl, A. W. Albrecht, S. M. G. Faeder, and D. M. Jonas, Chem. Phys. Lett. **297,** 307 (1998).
9. J. D. Hybl, A. A. Ferro, and D. M. Jonas, J. Chem. Phys. **115,** 6606 (2001).
10. P. F. Tian, D. Keusters, Y. Suzaki, and W. S. Warren, Science **300,** 1553 (2003).
11. A. A. Maznev, K. A. Nelson, and T. A. Rogers, Opt. Lett. **23,** 1319 (1998).
12. G. D. Goodno, G. Dadusc, and R. J. D. Miller, J. Opt. Soc. Am. B **15,** 1791 (1998).
13. Q. H. Xu, Y. Z. Ma, I. V. Stiopkin, and G. R. Fleming, J. Chem. Phys. **116,** 9333 (2002).
14. L. Lepetit, G. Cheriaux, and M. Joffre, J. Opt. Soc. Am. B **12,** 2467 (1995).
15. J. P. Likforman, M. Joffre, and V. Thierry-Mieg, Opt. Lett. **22,** 1104 (1997).
16. M. F. Emde, W. P. deBoeij, M. S. Pshenichnikov, and D. A. Wiersma, Opt. Lett. **22,** 1338 (1997).
17. S. M. Gallagher, A. W. Albrecht, T. D. Hybl, B. L. Landin, B. Rajaram, and D. M. Jonas, J. Opt. Soc. Am. B **15,** 2338 (1998).
18. C. Dorrer, N. Belabas, J. P. Likforman, and M. Joffre, J. Opt. Soc. Am. B **17,** 1795 (2000).
19. R. Trebino, K. W. DeLong, D. N. Fittinghoff, J. N. Sweetser, M. A. Krumbugel, B. A. Richman, and D. J. Kane, Rev. Sci. Instrum. **68,** 3277 (1997).
20. S. Mukamel, *Principles of Nonlinear Optical Spectroscopy* (Oxford U. Press, New York, 1995).
21. D. S. Larsen, K. Ohta, Q. H. Xu, M. Cyrier, and G. R. Fleming, J. Chem. Phys. **114,** 8008 (2001).
22. K. Ohta, D. S. Larsen, M. Yang, and G. R. Fleming, J. Chem. Phys. **114,** 8020 (2001).